Biochimica et Biophysica Acta 1802 (2010) 673–681

Contents lists available at ScienceDirect

Biochimica et Biophysica Acta

journal homepage: www.elsevier.com/locate/bbadis

Reduced creatine kinase as a central and peripheral biomarker in Huntington's disease

Jinho Kim [a,b], Daniel J. Amante [a,b], Jennifer P. Moody [a], Christina K. Edgerly [a], Olivia L. Bordiuk [a], Karen Smith [a,b], Samantha A. Matson [a], Wayne R. Matson [a], Clemens R. Scherzer [c], H. Diana Rosas [d,e], Steven M. Hersch [d,e], Robert J. Ferrante [a,b,*]

[a] Geriatric Research Education Clinical Center, New England Veterans Administration VISN 1, Bedford, MA 01730, USA
[b] Neurology, Laboratory Medicine and Pathology, and Psychiatry Departments, Boston University School of Medicine, Boston, MA 02118, USA
[c] Center for Neurologic Diseases, Brigham & Women's Hospital and Harvard Medical School, Cambridge, MA 02139, USA
[d] Neurology Service, Massachusetts General Hospital and Harvard Medical School, Boston, MA 02114, USA
[e] Mass General Institute for Neurodegenerative Disease, Massachusetts General Hospital, Charlestown, MA 02129, USA

ARTICLE INFO

Article history:
Received 1 March 2010
Received in revised form 13 April 2010
Accepted 3 May 2010
Available online 9 May 2010

Keywords:
Biomarker
Creatine kinase
Huntington's disease
Energetic defects
Blood buffy coat

ABSTRACT

A major goal of current clinical research in Huntington's disease (HD) has been to identify preclinical and manifest disease biomarkers, as these may improve both diagnosis and the power for therapeutic trials. Although the underlying biochemical alterations and the mechanisms of neuronal degeneration remain unknown, energy metabolism defects in HD have been chronicled for many years. We report that the brain isoenzyme of creatine kinase (CK-BB), an enzyme important in buffering energy stores, was significantly reduced in presymptomatic and manifest disease in brain and blood buffy coat specimens in HD mice and HD patients. Brain CK-BB levels were significantly reduced in R6/2 mice by ~18% to ~68% from 21 to 91 days of age, while blood CK-BB levels were decreased by ~14% to ~44% during the same disease duration. Similar findings in CK-BB levels were observed in the 140 CAG mice from 4 to 12 months of age, but not at the earliest time point, 2 months of age. Consistent with the HD mice, there was a grade-dependent loss of brain CK-BB that worsened with disease severity in HD patients from ~28% to ~63%, as compared to non-diseased control patients. In addition, CK-BB blood buffy coat levels were significantly reduced in both premanifest and symptomatic HD patients by ~23% and ~39%, respectively. The correlation of CK-BB as a disease biomarker in both CNS and peripheral tissues from HD mice and HD patients may provide a powerful means to assess disease progression and to predict the potential magnitude of therapeutic benefit in this disorder.
Published by Elsevier B.V.

1. Introduction

Huntington's disease (HD) is an autosomal dominant and fatal neurological disorder caused by an expanded trinucleotide CAG repeat in the gene coding for the protein, huntingtin. No proven treatment to prevent the onset or to delay the progression of HD currently exists. A major goal of current clinical research in HD is to develop biomarkers that detect and monitor progression of preclinical and early manifest disease in order to help facilitate clinical trials.

Despite great progress, a direct causative pathway from the HD gene mutation to neuronal dysfunction and death has not yet been established. There is strong evidence from human and animal studies, however, suggesting that one mechanism by which mutant huntingtin and its fragments trigger both damaging and compensatory molecular processes is via mitochondrial damage and energy depletion, ultimately leading to increasingly fragile neurons susceptible to more generic stresses and neuronal death [1]. Energetic defects in HD subjects have been chronicled for many years and include primary alterations of electron transport chain complexes [2–8]. A secondary consequence of the gene defect causing impaired energy metabolism is mitochondrial dysfunction. N-terminal huntingtin fragments may directly impair mitochondrial function, leading to increased oxidative damage [7]. Strong evidence also exists for early metabolic deficits and energy depletion in HD subjects, as early weight loss prior to the onset of chorea [9], reduced glucose utilization and hypometabolism in both presymptomatic and symptomatic HD patients prior to striatal atrophy [10,11], and magnetic resonance spectroscopy showing a significant decrease in the phosphocreatine to inorganic phosphate ratio in resting muscle and increased lactate concentrations in the cerebral cortex [12]. It is of interest to note that in patients with other trinucleotide repeat diseases, such as spinocerebellar ataxias, there is a common mechanism linking energy

* Corresponding author. Geriatric Research Education Clinical Center, New England Veterans Administration VISN 1, Bedford, MA 01730, United States. GRECC Unit 182B, Bedford VA Medical Center, 200 Springs Road, Bedford, MA 01730, USA. Tel.: +1 781 687 2908; fax: +1 781 687 3515.
E-mail address: rjferr@bu.edu (R.J. Ferrante).

0925-4439/$ – see front matter. Published by Elsevier B.V.
doi:10.1016/j.bbadis.2010.05.001

deficiency to the polyglutamine gene mutation [13,14]. There is also substantial evidence in experimental models of HD, suggesting an important interplay between energy metabolism defects and aberrant mitochondrial function in the pathogenesis of HD [15].

Creatine kinase (CK), an enzyme that rapidly catalyses the conversion of creatine and consumes adenosine triphosphate to create phosphocreatine and adenosine diphosphate, is an important enzyme in producing and buffering energy stores [16]. There are two subunits, B (brain type) and M (muscle type), with three different circulating isoenzymes, CK-MM, CK-BB and CK-MB [16,17]. In addition, there are two mitochondrial creatine kinase isoenzymes, the ubiquitous (uMT-CK) and sarcomeric form. ATP, the key energetic molecule, is tightly coupled to phosphocreatine metabolism via the CK enzyme system [16]. As such, CK plays a central role in energy transfer in cells with high and fluctuating energy requirements and is critically vital in energy homeostasis. CK isoenzymes are highly susceptible to oxidative stress [18], an important pathophysiological mechanism associated with HD [19]. Of note, CK-BB is specific to inhibitory neurons in the brain [20], those that selectively degenerate in HD [21].

While CK activity has been reported in moderate-late stage R6/2 mice [22], there are no studies that examine the early and progressive loss of CK in central nervous system and peripheral blood tissue specimens from HD patients, with correlation in HD mice. We investigated CK-BB in premanifest and symptomatic human HD patients with parallel studies in the fragment R6/2 and the full-length 140 CAG knock-in models of HD mice. We hypothesize that decreased brain energetics in HD may be the result of reduced activity of the CK system and that early loss of CK-BB may be an important unrecognized biomarker of disease.

2. Methods

2.1. R6/2 and 140 CAG mouse samples

Male transgenic fragment R6/2 and heterozygous full-length 140 CAG knock-in mice were obtained from established colonies at the Bedford VA Medical Center and were backcrossed with B6CBA females from Jackson Laboratory (Bar Harbor, ME). The offspring were genotyped using a PCR assay on tail DNA. Cohort homogeneity is essential in testing potential hypotheses in murine models of disease. Minimizing measurement variability increases the power to detect differences. Mice were randomized from approximately 50 litters all within 4 days of the same age from the same 'f' generation of R6/2 and 140 CAG mice. Any mice that had altered CAG repeats outside of the expected range from both R6/2 mice (148–153 CAG repeats) and 140 CAG mice (138–143 CAG repeats) were excluded from the study, since increased or reduced CAG repeats outside of the expected range may result in increased variability in disease severity [23]. Mice were equally distributed according to weight and parentage within each cohort ($n=10$) of R6/2 and 140 CAG mice and littermate age-matched wild type control mice. Since others and we have not observed gender differences in the R6/2 and 140 CAG HD mice, female mice were used in the experimental paradigms. The mice were housed five in each cage under standard conditions with *ad libitum* access to food and water. Mice were identified by a randomly assigned code so that the studies were performed blind as to the genetic identity of the mice. The mice were handled under the same conditions by one investigator. Groups ($n=10$) of mice were euthanized by decapitation at 21, 30, 63, and 91 days of age from R6/2 mice and at 2, 4, 8, and 12 months of age from 140 CAG mice. This allows for an analysis across the clinical spectrum of disease severity in each HD mouse model from clinically premanifest time points, disease onset, mid stage disease, and late stage disease. Fresh blood (0.3–0.5 ml) was collected in Eppendorf tubes containing 0.05 ml heparin, immediately centrifuged to separate blood components, frozen in liquid nitrogen (−80°C), and stored in a −80°C freezer for subsequent analysis. Brains were rapidly dissected, quartered, placed in Eppendorf tubes, flash frozen in liquid nitrogen (−80°C), and stored at −80°C. From decapitation to freezing of brain tissue and blood specimens took no more than 70 s with a team of four investigators. Our experience has been that longer dissection times result in increasing variability in the data that precludes significance.

Groups ($n=10$) of R6/2 and 140 CAG mice and littermate wild-type control mice from the late stage time points were deeply anesthetized and transcardially perfused with 2% buffered paraformaldehyde (100 ml), with care to avoid the introduction of any perfusion artifact. Brains were removed, cryoprotected, and serially sectioned (50 μm). Serial cut mouse tissue sections were subsequently immunostained for CK-BB. All of the experiments were performed in accordance with the National Institutes of Health Guide for the Care and Use of Laboratory Animals and were approved by both the Veterans Administration and Boston University Animal Care Committees.

2.2. Human samples

Postmortem striatal tissue specimens from 22 adult-onset HD patients (five Grade 2 cases, nine Grade 3 cases, and eight Grade 4 cases; mean age of death, 67.1 years; range, 59–70 years) and eight age-matched patients without any known neurological sequela (mean age, 68.9 years; range 60–78 years) were dissected fresh and rapidly quenched in liquid nitrogen (−80°C). Brain tissue specimens were collected at the Bedford Veterans Administration Medical Center Brain Tissue Archive and the Boston University Alzheimer's Disease Center. The postmortem intervals did not exceed 18 h (mean time, 12.2 h; range, 4–14 h) and were similar for controls and HD patients. CAG repeat length analysis was performed on the HD specimens (mean number of CAG repeats, 44.2). The range of CAG repeats in the adult-onset HD patients was 41–46. Each HD patient had been clinically diagnosed based on known family history and phenotypic symptoms of HD. The diagnosis of HD was confirmed by neuropathological examination and graded by severity [24]. Blood was collected into heparin tubes and processed to obtain buffy coats from 30 HD subjects and 20 controls and flash frozen *in situ* undisturbed by pipetting. The blood samples were collected for the REVEAL-HD biomarker project at the Massachusetts General Hospital Huntington's Disease Center (HDR and SMH) under an IRB approved protocol. Subjects included presymptomatic individuals known to possess the genetic mutation causing HD, individuals with symptomatic HD, and spousal controls.

As with the mouse samples, paraformaldehyde–lysine–periodate fixed striatal tissue blocks from 10 Grade 3 and 8 age-matched non-neurological controls were rinsed in 0.1 M sodium phosphate buffer, and placed in cold cryoprotectant in increasing concentrations of 10% and 20% glycerol, 2% DMSO solution for 24–36 h. Frozen serial sections of the striatal tissue blocks from the anterior commissure to the rostral extent of the globus pallidus were cut at 50-μm intervals in the coronal plane and placed within a six-well collection container. The cut sections were stored in 0.1 M sodium phosphate buffer with 0.08% sodium azide at 4 °C for subsequent immunocytochemistry using a CK-BB antibody (1:500, Abcam).

2.3. Western blot analysis, brain

Brain lysates from both human patients and HD mice were obtained by fractionating striatal tissue samples in 100 mM Tris (pH 7.4) buffer containing 1% Triton-X 100, 150 mM NaCl, 1 mM sodium orthovanadate, 5 mM sodium fluoride, 3 mM PMSF, 3 mM DTT, 0.5 μg/ml leupeptin, and 10 μg/ml aprotinin. Thirty micrograms of protein from tissue lysates from the medial caudate nucleus in patients and the left frontal neostriatum in HD mice was electrophoresed under reducing conditions on 8% polyacrylamide gels. Proteins were transferred to a nitrocellulose membrane (Bio-Rad, Hercules, CA). Nonspecific binding was inhibited by incubation in

Table 1
Data analysis of brain and blood samples from R6/2 HD mice measuring Ck-BB levels.

Days	Brain					Blood				
	R6/2	±	WI	±	$p<0.05$	R6/2	±	WI	±	$p<0.05$
21 days	0.613	0.035	0.752	0.029	0.047	0.447	0.033	0.522	0.023	0.047
30 days	0.688	0.051	0.83	0.021	0.013	0.456	0.041	0.54	0.021	0.022
42 days	0.564	0.059	0.85	0.018	0.001	0.433	0.053	0.581	0.018	0.017
63 days	0.331	0.047	0.946	0.038	0.001	0.398	0.061	0.632	0.038	0.001
91 days	0.287	0.038	0.912	0.021	0.001	0.346	0.057	0.617	0.026	0.001

Tris-buffered saline (TBST; 50 mM Tris–HCl, pH 8.0, 0.9% NaCl, and 0.1% Tween 20) containing 5% nonfat dried milk for 0.5 h. Primary antibodies against CK-BB isoenzyme (1:1000, Abcam, USA) were diluted at 1:1000 in TBST with 1% milk and exposed to membranes overnight at 4 °C. The membrane was washed twice in TBS-T 10 min each, incubated in secondary antibodies (1:3000 goat anti rabbit for CK-B) and 1:5000 goat anti mouse for alpha tubulin), and washed three times in TBS-T. Immunoreactive proteins were detected according to the enhanced chemiluminescence protocol (Pierce Biotechnology, Rockford, IL). Results were standardized to alpha tubulin and analyzed using NIH Image.

2.4. Dot blot analysis, buffy coat

Buffy coat samples from both patients and mice were analyzed for CK-BB. The dissection of blood buffy coats is critical to the success of the method and must be precise. Introducing serum or RBCs within the sample alters the results, causing increased variability and reduced significance. Tissue samples were placed in 300 µl Tris lysis buffer (pH 7.4) containing 3.5 mM NaCl, 0.5% EDTA, 2.5 mM NP40, 10 µg/ml $NaVO_4$, and 200 mM PMSF. Proteins were transferred to a nitrocellulose membrane (Bio-Rad, Hercules, CA), with light vacuum applied to the membrane for 1 h in a dot blot apparatus. The membrane was rinsed in TBS-T for 10 min, blocked with 5% milk in TBS-T and 1:1000 sodium azide for 2 h at room temperature and then incubated with primary antibody overnight at 4 °C. The membrane was washed twice in TBS-T 10 min each, incubated in secondary antibodies (1:3000 goat anti rabbit for CK-BB and 1:5000 goat anti mouse for alpha tubulin) ,and washed three times in TBS-T, incubated in chemiluminescent reagent 5 min, blotted, exposed to film, and developed. The optical density of immunoblots was measured using a computer-based image analysis system (NIH Image) and standardized to alpha tubulin. Densitometric analysis was performed with the experimenter (JK and RJF) blinded to disease conditions on multiple rendered images. Of interest to note is that hospital lab testing for CK is not specific for isoenzyme type and measures total enzyme activity.

2.5. Behavioral testing (open field testing)

Behavioral testing for 140 CAG mice was performed during the light phase of the diurnal cycle since these mice are sufficiently active during that time. Measurements were made for 30 min after 15 min of acclimation to the box (Opto-Varimex Unit, Columbus Instruments, Columbus, OH, USA). Counts of horizontal and vertical motion activity were monitored and quantitative analysis of locomotor activity and rearing were assessed. The open field box was cleaned before testing each mouse. Each 30 min of testing were analyzed as three periods of 10-min intervals to study the influence of novelty and measured behavior. The position of the cage in the array was kept constant throughout testing. Any beam interruption was recorded and processed by the Auto-Track System (ATS) software. The ATS software recorded four separate measures: total ambulatory counts; total resting time, ambulatory time, and total distance traveled. Mice were coded and investigators were blinded to the genotype and analysis.

2.6. Immunocytochemistry

Immunohistochemical localization of the CK-BB antibody (1:500, Abcam, USA) was performed by using a conjugated second antibody

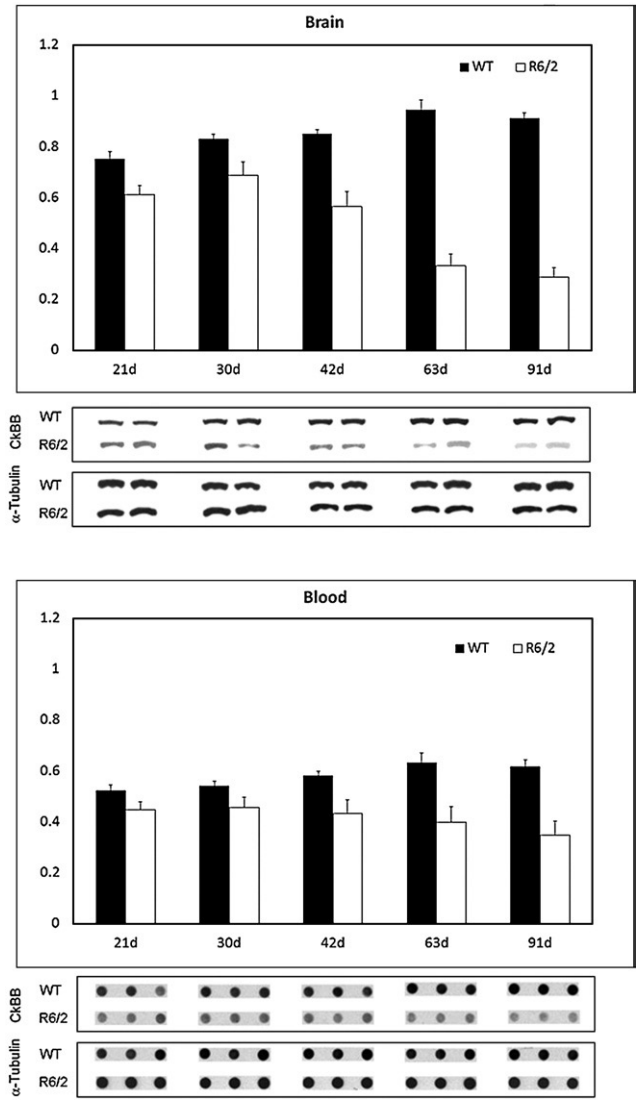

Fig. 1. Western and dot blot analyses of brain and blood from R6/2 HD mice through the spectrum of disease at a premanifest stage (21 days), onset (30 days), and though early (42 days), moderate (63 days), and end stage disease (91 days). There were significant differences between mutant and littermate control mice at each disease stage, to include premanifest disease (Table 1). Blots are shown under each time point with alpha tubulin controls.

method. Tissue sections from human and mouse striata were preincubated in an absolute methanol and 0.3% hydrogen peroxide solution for 30 min, washed (three times) in PBS (pH 7.4) for 10 min each, placed in 10% normal goat serum (GIBCO) for 1 h, incubated free-floating in primary antiserum at room temperature for 12–18 h (all dilutions of primary antisera above included 0.08% Triton X-100 and 2% normal goat serum), washed (three times) in PBS for 10 min each, placed in horse radish peroxidase-conjugated goat anti-rabbit IgG (1:300 in PBS, Boehringer Mannheim, Indianapolis) or goat anti-mouse IgG (1:300 in PBS, Boehringer Mannheim), washed (three times) in PBS for 10 min each, and reacted with 3,3'-diaminobenzidine HCl (1 mg/ml) in Tris–HCl buffer with 0.005% hydrogen peroxide. Specificity for the antisera used in this study was examined in each immunochemical experiment to assist with interpretation of the results. This examination was accomplished by omission of the primary and secondary antibodies to determine the amount of background generated from the detection assay.

2.7. Fluorescent immunocytochemistry

Combined immunofluorescence staining for GFAP and CK-BB was performed on human striatal HD and normal control tissue specimens. Striatal sections were incubated with rabbit anti-CK-BB antibody (1:500, Abcam, USA) and mouse ant-GFAP antibody (1:500, Chemicon, USA) in Tris–HCl buffer containing 0.3% Triton X-100 for 24–72 h at 4 °C. Sections were then rinsed 3 times in PBS, incubated in the dark with goat anti-rabbit Cy3 conjugate (1:200, Jackson Labs, USA) and goat anti-mouse FITC conjugate (1:200, Vector, USA) for 2 h at 20 °C. After rinsing three times in PBS, sections were wet-mounted and coverslipped with 50% glycerol. Identical microscopic fields were immediately photographed with a Nikon Eclipse E800 fluorescent microscope, delineating the location of GFAP and CK-BB immunoreactivities within the same striatal section. The fields were merged and colocalization was analyzed.

2.8. Analysis

Multiple data sets were generated for each premanisfest and manifest CK-BB biomarker profile in mice and human subjects. Interval scale data involving multiple groups were analyzed using ANOVA and repeated measures of ANOVA, with multiple comparisons performed using Fishers least significant difference test. This data was correlated and explored together from both the human and mouse profiles. Statistical analyses of biomarker data focused on the differences between groups and changes in the values of the biomarkers over time with clinical measures of disease progression.

3. Results

An analysis of R6/2 and 140 CAG HD mice showed a significant reduction in CK-BB levels in both brain and blood buffy coat samples that were disease severity dependent in each mouse model. In R6/2 HD mice, brain levels of CK-BB were significantly reduced in premanifest diseased mice at 21 days by 18.5% (Table 1, Fig. 1). There was an increasing loss of CK-BB levels through early, moderate, and severe disease stages through 91 days of age, reaching a 68.5% loss of brain CK-BB levels, as compared to littermate wild type control mice (Table 1, Fig. 1). Consistent with a disease-dependent loss of brain CK-BB, significant reductions in CK-BB were observed in blood buffy coat samples in presymptomatic mice and throughout disease progression (Table 1, Fig. 1). The loss of CK-BB in blood samples was not as great as that observed in brain samples and ranged from 14.4% in premanifest diseased R6/2 mice to 43.9% in severe stage disease at 91 days. Immunohistological studies of cut brain tissue sections at the level of the neostriatum showed parallel changes in CK-BB loss that was most apparent at 91 days, with reduced immunoreactivity in both the neuropil and cytoplasm of neurons (Fig. 2).

In contrast, CK-BB levels in both brain and blood buffy coat tissue samples were not significantly reduced at the earliest time point

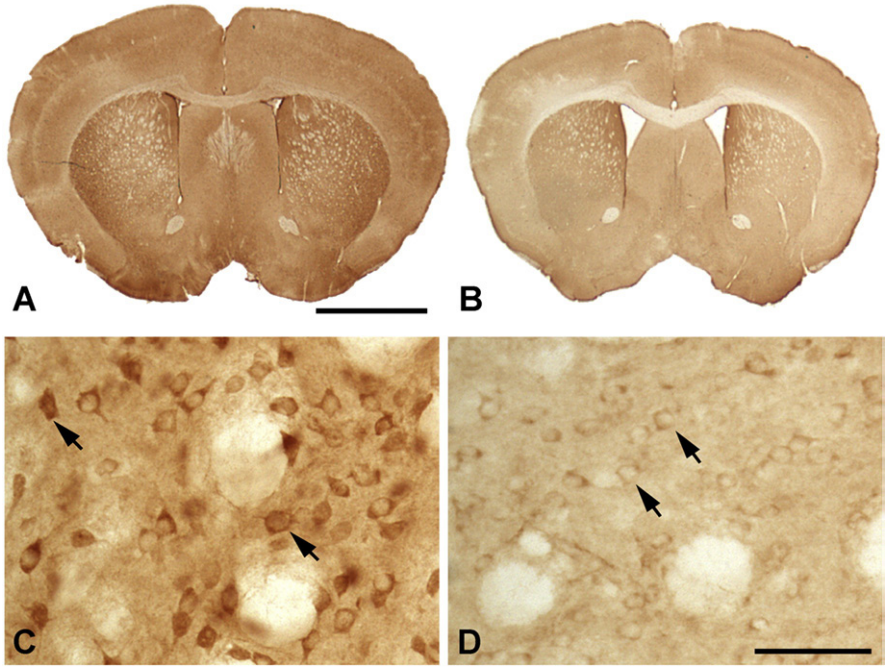

Fig. 2. CK-BB immunohistochemistry of brain sections through anterior neostriatum at the level of the anterior commissure in R6/2 mice at 91 days. Gross CK-BB immunoreactivity is reduced in the R6/2 mutant mouse (B), in comparison to the wild type littermate control (A). Higher magnification of the neostriatum from each tissue section shows a marked reduction in CK-BB immunoreactivity in the mutant R6/2 mouse (D) within both the neuropil and the cytoplasm of striatal neurons (arrows), as compared to the wild type littermate control mouse (C). Magnification bar in A is 2 mm. Magnification bar in D is 100 μm.

(2 months) in 140 CAG full-length HD mice, as compared to littermate control mice. Significant losses of brain CK-BB levels, however, were present at 4-, 6-, 8-, and 12-month time points in a severity of disease-dependent manner, ranging from 18.9% to 41.9% (Table 2, Fig. 3). Congruous with brain CK-BB levels, CK-BB levels in blood buffy coat samples were also significantly reduced with increased disease severity and similar percentile levels of loss from 17.8% to 41.4% (Table 2, Fig. 3). While previous hyperkinetic motor activity has been observed at 1 month of age and hypoactivity at 4 months [25], our open field analyses in 140 CAG mice of distance traveled, ambulatory counts, resting time, and ambulatory time showed significant differences from only the 3 month time point onward ($p<0.5$), in comparison to littermate control mice (Fig. 4), suggesting that the 2-month time point may be a clinically premanifest time point. Immunostaining of 140 CAG mice tissue sections using CK-BB antisera confirmed CK-BB loss in the brain, showed reduced gross CK-BB immunoreactivity and a loss of CK-BB within the neuropil and in the cytoplasm of neurons (Fig. 5).

We evaluated CK-BB in human HD brain and blood buffy coat specimens by using well-defined HD stages of disease. CK-BB was reduced in a grade-dependent manner in caudate nucleus specimens of all grades of severity (Grades 2–4) from HD patients, as compared to non-diseased control tissue specimens (Fig. 6). Densitometric analysis showed significantly reduced differences between CK-BB levels with increasing grade of severity [24] (Control vs. G2: 27.6%, $p<0.04$; Control vs. G3; 53.4%, $p<0.001$; Control vs. G4: 63.4%, $p<0.0001$) (Table 3, Fig. 6). In addition, there were significant differences between each HD grade (G2 vs. G3; 35.6%, $p<0.001$; G3 vs. G4: 21.5%, $p<0.01$) (Table 3, Fig. 6). Blood buffy coat specimens showed a significant loss of CK-BB levels in both premanifest (22.6%, $p<0.01$) and manifest (38.5%, $p<0.001$) HD patients, with a greater loss in manifest disease samples (Table 3, Fig. 6). CK-BB immunostaining in 50-μm-thick tissue sections confirmed the findings of reduced CK-BB levels in HD striatal specimens (Fig. 7). There was reduced CK-BB immunoreactivity in the HD neostriatum. While cytosolic CK-BB immunoreactivity was markedly reduced in neurons, intense CK-BB immunostaining was present in astrocytes in HD tissue sections (Fig. 7B and D). Combined immunofluorescence for GFAP and CK-BB immunoreactivities confirmed this observation (Fig. 7E, F and G). The latter is most likely the consequence of increased reactive astrogliosis, a hallmark pathological phenomenon in the neostriatum of HD subjects [24]. Of note, the expression of CK-BB in mice is predominantly found in astrocytes and cortical inhibitory neurons in mice [20]. The expression of CK correlates with L-arginine:glycine amidinotransferase (AGAT) and guanidinoacetate methyltransferase (GAMT), two enzymes responsible for creatine biosynthesis [20]. As such, any alteration in these enzymes in HD may impact disease expression. In patients with GAMT and AGAT mutations, clinical symptoms include mental and motor retardation, extra-pyramidal symptoms, and seizures [26,27]. Braissant and colleagues [28] have recently suggested that there is a dissociation between GAMT and AGAT activities in neurons, with only GAMT expression in the neostriatum. A GAMT deficiency may result in reduced CK and creatine deficiencies in HD, with subsequent impaired energetics and neurodegeneration.

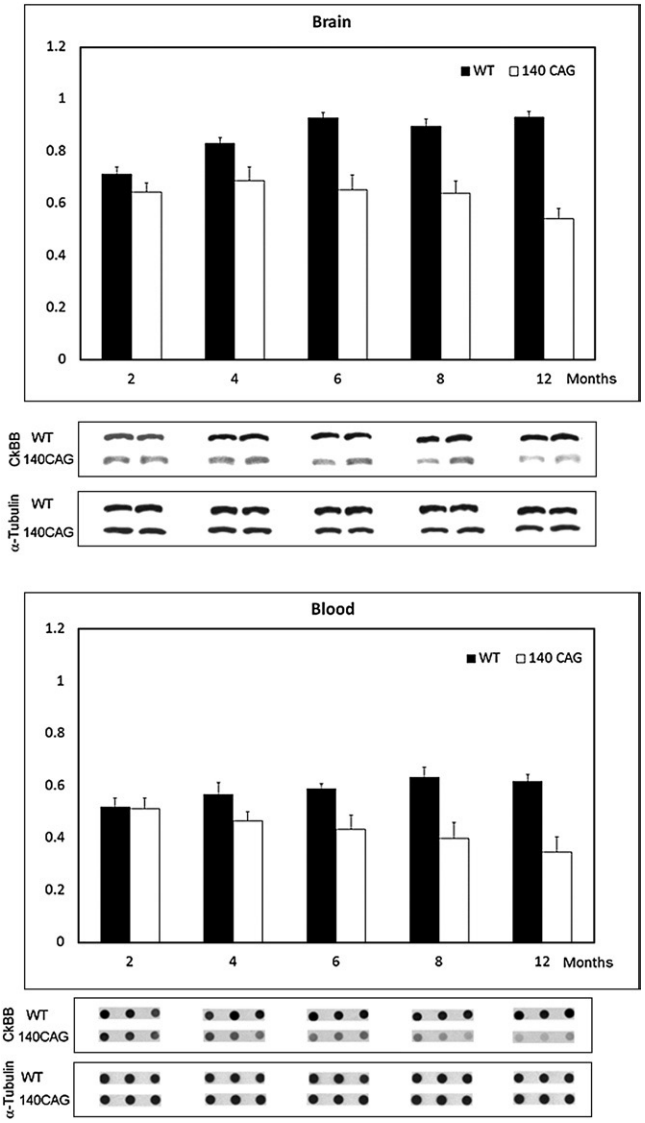

Fig. 3. Western and dot blot analyses of brain and blood from 140 CAG HD mice through the spectrum of disease at a premanifest stage (2 months), onset (4 months), though early (6 months), moderate (8 months), and severe disease (12 months). There were significant differences between mutant and littermate control mice at each disease stage starting a 4 months of age (Table 2). Blots are shown under each time point with alpha tubulin controls.

4. Discussion

Creatine kinase (CK) catalyzes the reversible transfer of a phosphoryl group from phosphocreatine PCr to adenosine diphosphate (ADP), forming adenosine triphosphate (ATP). Thus, creatine kinase offsets energy depletion by forming PCr, providing a spatial

Table 2
Data analysis of brain and blood samples from 140 CAG HD mice measuring Ck-BB levels.

Months	Brain					Blood				
	140 CAG	±	WT	±	$p<0.05$	140 CAG	±	WT	±	$p<0.05$
2	0.643	0.035	0.712	0.029	0.069	0.51	0.042	0.519	0.033	0.431
4	0.688	0.051	0.83	0.021	0.013	0.466	0.035	0.567	0.044	0.02
6	0.653	0.056	0.928	0.02	0.005	0.433	0.053	0.589	0.018	0.01
8	0.639	0.047	0.895	0.028	0.009	0.398	0.061	0.632	0.038	0.001
12	0.541	0.04	0.931	0.021	0.001	0.346	0.057	0.617	0.026	0.001

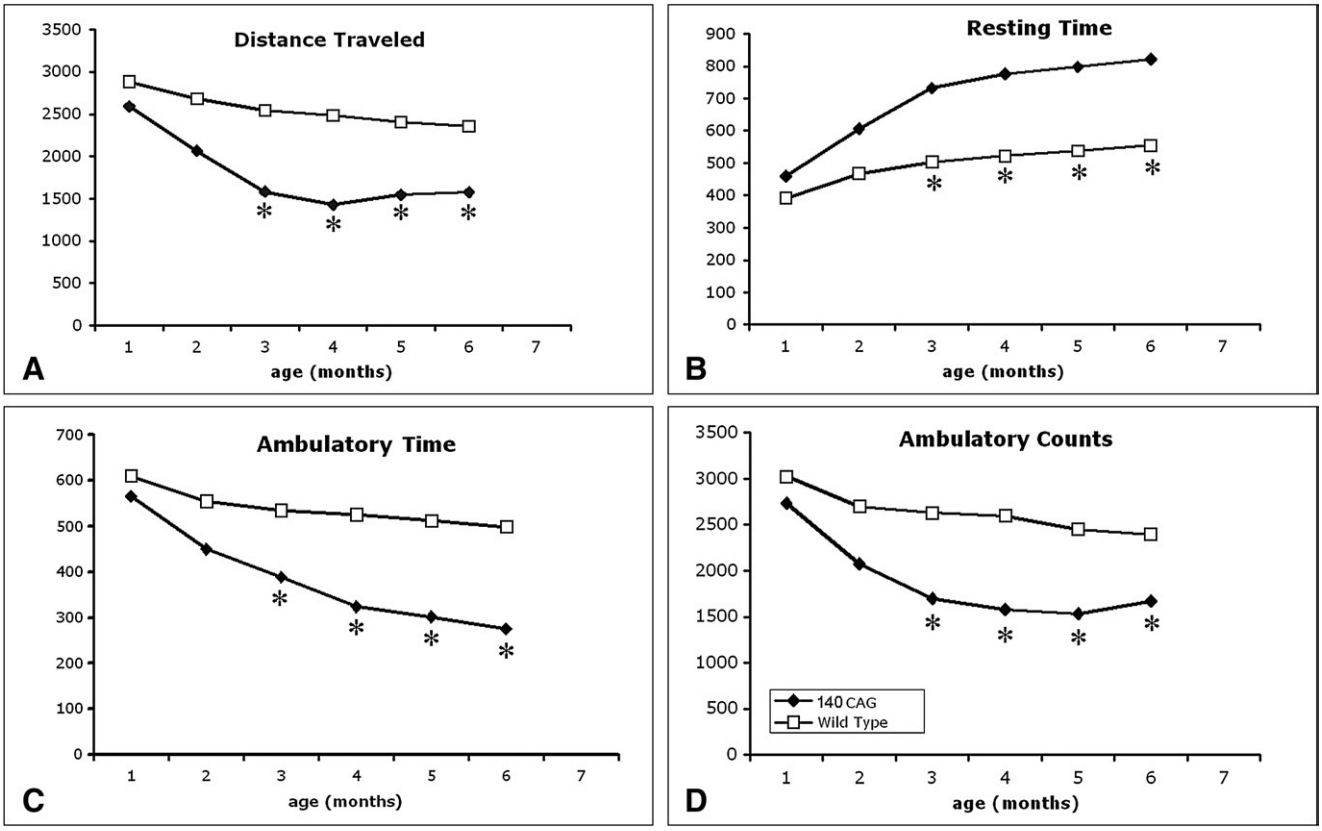

Fig. 4. Open field analysis of 140 CAG full-length mutant HD mice from 1 to 6 months. There are significant differences in distance traveled (A), resting time (B), ambulatory time (C), and ambulatory counts (D) starting at 3 months of age. Significance was not obtained at 1 and 2 months. $^{*}p<0.05$.

energy buffer to re-phosphorylate ADP to ATP at cellular sites of energy consumption and, in the reversible reaction, forming PCr and ADP from creatine and ATP at cellular sites of high-energy phosphate production (PCr shuttle hypothesis) [29–32]. As such, CK is critically vital to cellular energy homeostasis and its loss may result in reduced energy stores and subsequent neuronal dysfunction and death in HD. It is of interest to note that CK-BB knockout mice present with pathological sequelae of reduced body and brain weight, atrophied

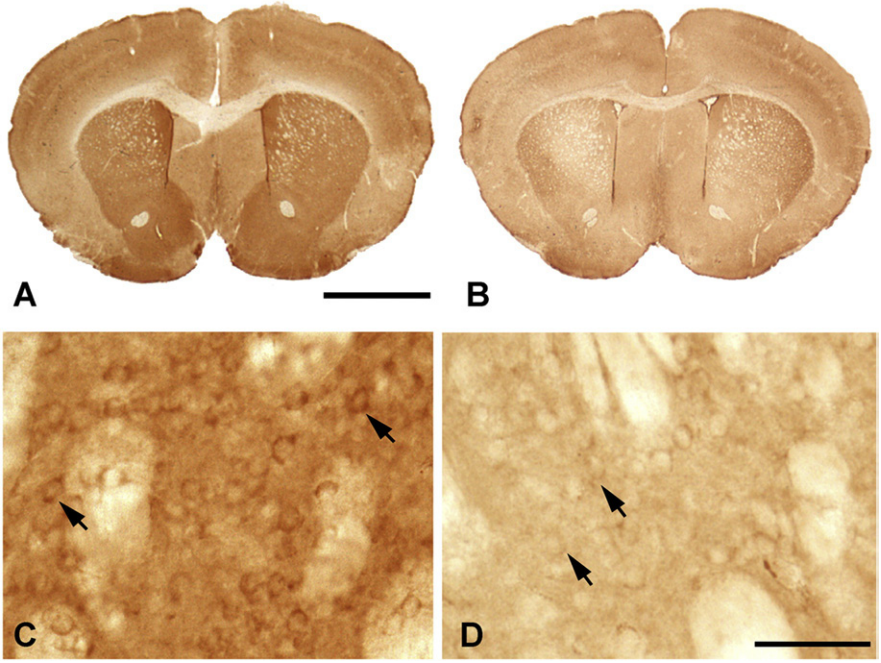

Fig. 5. CK-BB immunohistochemistry of brain sections through the anterior neostriatum at the level of the anterior commissure in 140 CAG HD mice at 8 months. Gross CK-BB immunoreactivity is reduced in the 140 CAG mutant mouse (B), in comparison to the wild type littermate control mouse (A). Higher magnification within the neostriatum from each tissue section shows a reduction in CK-BB immunoreactivity in the mutant 140 CAG mouse (D) within both the neuropil and the cytoplasm of striatal neurons (arrows), as compared to the wild type littermate control mouse (C). Magnification bar in A is 2 mm. Magnification bar in D is 100 μm.

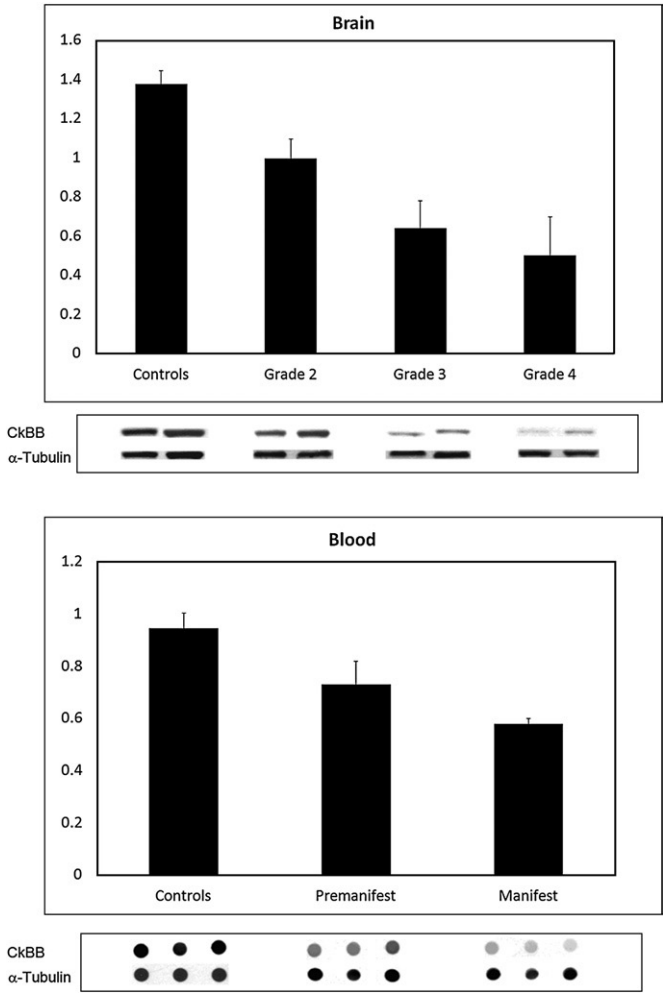

Fig. 6. Western analysis from the medial segment of the caudate nucleus (brain) of age-matched control patients and Grade 2, Grade 3, and Grade 4 HD patients. There was a significant grade-dependent reduction in CK-BB, with the greatest loss in Grade 4 HD (Table 3). Blood buffy coat CK-BB analysis from age-matched patient caregivers and premanifest and manifest HD patients showed a significant loss of CK-BB in both premanifest disease and manifest diseased HD patients, as compared to the controls (Table 3). Blots are shown under each time point with alpha tubulin controls.

hippocampi, hyperventricular enlargement, and impaired spatial learning [33,34], all consistent with neurodegenerative effects found in both HD mouse models and HD patients [1,15,35]. Our results provide supporting evidence of mitochondrial damage and impaired energy metabolism in HD [36]. The fact that CK-BB levels are significantly reduced in both brain and peripheral blood buffy coat samples from HD mice and HD patients at premanifest and manifest disease stages are of additional significance, especially since CK-BB may be a potential peripheral biomarker for this neurological disorder.

While it is to be expected that the brain is altered in a neurodegenerative disorder, it may not be as obvious that biomarkers of HD could be found in peripheral tissue samples such as blood, as it is a central nervous system disorder. For a peripheral biomarker to represent the "state" of HD, it would either have to be derived from the brain or represent pathology occurring in the periphery. The mutant huntingin protein is expressed ubiquitously throughout the body, including blood, and may cause detectable, but clinically silent changes in gene expression and biochemistry anywhere [35]. It is important to understand what relation potential peripheral biomarkers would have to neurodegeneration in the brain. By using HD mice in these studies, we examined complementary processes in the brain and periphery with much greater precision and much greater control of post-mortem and other technical factors associated with human tissue sampling. The present findings suggest that CK-BB levels could serve as a biomarker of disease progression in premanifest and in manifest disease HD patients. We are currently further investigating CK-BB levels in blood samples from human clinical trials in HD patients to assess its potential as a pharmacodynamic marker.

Table 3
Data analysis of brain and blood samples from HD patients measuring CK-BB levels.

Brain		±	$p<0.05$	Blood		±	$p<0.05$
Controls	1.376	0.068		Controls	0.946	0.057	
Grade 2	0.995	0.102	0.04	Premanifest	0.732	0.088	0.01
Grade 3	0.641	0.139	0.001	Manifest	0.581	0.018	0.001
Grade 4	0.503	0.196	0.0001				

Although tremendous efforts have been made in recent years to identify early genetic, clinical, and biochemical biomarkers that indicate the presence of disease prior to the onset of clinical expression in neurodegenerative disorders, specific biomarkers for premanifest HD are very limited at the present time [37]. We have, however, characterized one biomarker, 8-hydroxy-2'-deoxyguanosine (a marker of DNA oxidation), in urine, blood, and brain in manifest HD patients with correlation in HD mice that acts as a marker of disease progression and therapeutic efficacy [38–40]. Elevated central and peripheral levels of 8-hydroxy-2'-deoxyguanosine are not specific to HD. Others and we have found elevated levels of 8-hydroxy-2'-deoxyguanosine in other neurodegenerative disorders and experimental models of neurological diseases, such as amyotrophic lateral sclerosis, Parkinson's disease, and Alzheimer's disease [38,39,41–45]. Similarly, reduced levels of CK-BB are not specific to HD alone. We have novel preliminary evidence that CK-BB is also significantly reduced in spinal cord samples and in blood buffy coat samples from sporadic amyotrophic lateral sclerosis patients.

Biomarkers provide a diagnostic tool to improve early detection of disease in at-risk individuals and provide greater diagnostic accuracy. Since there may be a prolonged period of time in which neurons become dysfunctional before clinical expression of disease, preclinical detection of biomarkers offers the promise of administering disease-modifying medications during the premanifest period, further delaying or ameliorating disease symptoms than treatment after disease onset. CK-BB may act as a "predictor" in defining surrogate endpoints that substitute for a true clinical outcome endpoint for the purpose of comparing specific interventions or treatments in HD clinical trials. CK-BB may greatly facilitate the accurate evaluation of the effectiveness of new therapies and improve the safety and efficiency of clinical trials. While CK, also known as creatine phosphokinase (CPK), is often determined routinely in patients, this blood test is not specific for the type or isoenzyme of CK and measures total enzyme activity. Because CK enzymatic activity is measured under strict conditions of temperature, pH, substrate concentrations and activators, we are currently investigating direct assay of CK-BB in blood from HD patients to confirm the Western analyses.

A major advance in studying HD has been the development of both transgenic and full-length knock-in mouse models that exploit the mutation shown to underlie HD and replicate the clinical and neuropathological phenomena observed in HD patients [15,35,46]. One complementary research strategy has been to perform parallel correlative studies in human and animal models of disease in order to take advantage of advances being made in animal models and to best understand the most effective therapeutic strategies. Although logical and attractive, the validity of this approach remains to be proven. The HD mice have, however, identified a growing number of potential therapies that are in early phase human trials [1,47]. Genetic animal models of inherited neurological diseases provide an experimentally accurate system to identify the basis of molecular pathogenesis and provide an opportunity to test potential treatments and explore their

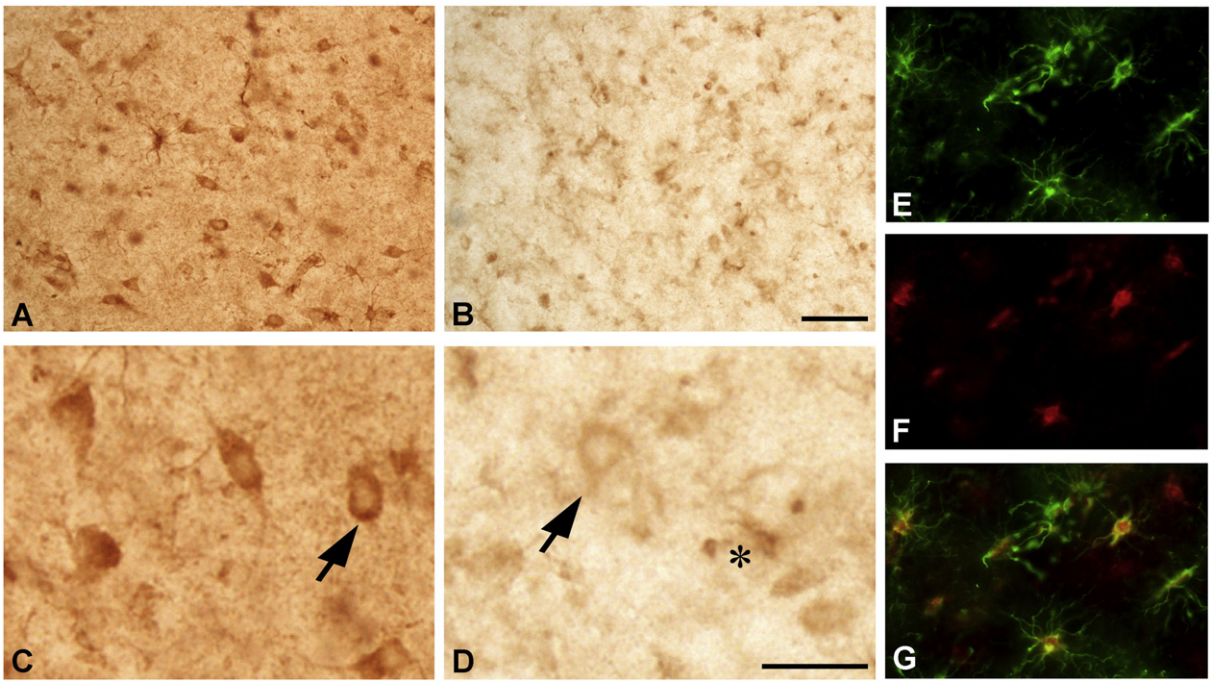

Fig. 7. CK-BB immunohistochemistry in the medial caudate nucleus from age-matched non-diseased control (A and C) and Grade 3 HD patient. There is marked loss of CK-BB immunoreactivity in HD (B and D), as observed in both low and high power magnification. CK-BB immunoreactivity is reduced within both the neuropil and the cytoplasm of striatal neurons (arrows), as compared to the control patient (A and C), with intense immunostaining in astrocytes in the HD specimen (asterisk in D). Combined GFAP and CK-BB immunofluorescence in the striatum from the same Grade 3 HD patient shows definitive colocalization of these proteins in astrocytes. Two-dimensional analysis showed overlap of each of the antisera [GFAP, green (E); CK-BB. Red (F); and merged figures (G)]. Magnification bar in A is 100 μm. Magnification bar in E is 50 μm.

promise for translation to humans experiencing HD. While both the transgenic fragment models and full-length knock-in models of HD share features with human HD [15], the degree of similarity to human HD increases the closer the model reproduces the exact genetic conditions for HD. As such, the full-length knock-in HD mice may provide the best possible molecular genetic comparability to human HD, especially prior to disease onset. The fulminant and early expression of disease in the R6/2 mice may not clearly estimate the degree of premanifest and early symptomatic identification of biomarkers, although others also report very early clinical phenomena in the full-length 140 CAG HD mice [25]. It is of interest to note, however, while the CK-BB levels were not significantly reduced in the 140 CAG mice at 2 months, there was a significant loss of CK-BB levels in premanifest HD patients.

Strong evidence supports the importance of the creatine kinase system and specific isoenzymes in neurodegenerative diseases [48,49] and the neuroprotective effect of creatine supplementation in studies of HD, amyotrophic lateral sclerosis, Parkinsonism, brain ischemia, and other neurological conditions [50]. Creatine is involved in regulating the octameric form of creatine kinase and decreases mitochondrial swelling when inhibitors of creatine kinase octamer–dimer transition are present [49,51]. Reduced creatine stores in HD may precipitate altered creatine kinase levels [50]. Energy is critical to the biological and molecular regulation of multiple cellular functions. As such, reduced energy levels, as a consequence of creatine kinase dysfunction or loss, threaten cellular homeostasis and integrity, resulting in subsequent neuronal death [48]. The present findings support the involvement of the creatine kinase system in HD. We have evidence that chronic high-dose creatine supplementation in both R6/2 and 140 CAG HD mice normalizes the reduced levels of CK-BB in both brain and blood buffy coat specimens in manifest disease (unpublished data). The present findings justify the ongoing clinical trials using high-dose creatine in HD patients. Interestingly, the neuroprotective effects of creatine may be creatine kinase isoenzyme-dependent, since creatine administration does not inhibit the mitochondrial transition pore in brain mitochondria with native mitochondrial creatine kinase [51,52].

Correlative analyses in brain and blood in both mice and man provide a powerful strategy for identifying potential peripheral biomarkers for HD. The present findings support the hypothesis of impaired energy metabolism in HD, identify a specific mechanism of energy compromise in the reduction of CK-BB, establish CK-BB as a potential biomarker of both central and peripheral premanifest and manifest disease, and provide further rationale for creatine as a potential neuroprotective treatment for HD.

Acknowledgments

We wish to thank Dr. Ann McKee for donating brain tissue specimens from the Boston University Alzheimer's Disease Brain Bank (NIA P30AG13846). This work was supported by National Institutes of Health Grants NS045806 (RJF and SMH), U01AT000613 (SMH) and NS058793 (SMH, HDR, CRS, WRM, RJF), the Veterans Administration VISN 1 (RJF and WRM), the New England HDSA Center of Excellence (SMH and HDR), and the CHDI Foundation (RJF).

References

[1] E.C. Stack, R.J. Ferrante, Huntington's disease: progress and potential in the field, Expert Opin Investig Drugs 16 (2007) 1933–1953.
[2] W.A. Brennan Jr., E.D. Bird, J.R. Aprille, Regional mitochondrial respiratory activity in Huntington's disease brain, J Neurochem 44 (1985) 1948–1950.
[3] W.D. Parker Jr., S.J. Boyson, A.S. Luder, J.K. Parks, Evidence for a defect in NADH: ubiquinone oxidoreductase (complex I) in Huntington's disease, Neurology 40 (1990) 1231–1234.
[4] V.M. Mann, J.M. Cooper, F. Javoy-Agid, Y. Agid, P. Jenner, A.H. Schapira, Mitochondrial function and parental sex effect in Huntington's disease, Lancet 336 (1990) 749.
[5] S.E. Browne, M.F. Beal, The energetics of Huntington's disease, Neurochem Res 29 (2004) 531–546.

[6] M. Gu, M.T. Gash, V.M. Mann, F. Javoy-Agid, J.M. Cooper, A.H. Schapira, Mitochondrial defect in Huntington's disease caudate nucleus, Ann Neurol 39 (1996) 385–389.
[7] A.V. Panov, C.A. Gutekunst, B.R. Leavitt, M.R. Hayden, J.R. Burke, W.J. Strittmatter, J.T. Greenamyre, Early mitochondrial calcium defects in Huntington's disease are a direct effect of polyglutamines, Nat Neurosci 5 (2002) 731–736.
[8] R.L. Albin, J.T. Greenamyre, Alternative excitotoxic hypotheses, Neurology 42 (1992) 733–738.
[9] L. Djousse, B. Knowlton, L.A. Cupples, K. Marder, I. Shoulson, R.H. Myers, Weight loss in early stage of Huntington's disease, Neurology 59 (2002) 1325–1330.
[10] D.E. Kuhl, C.H. Markham, E.J. Metter, W.H. Riege, M.E. Phelps, J.C. Mazziotta, Local cerebral glucose utilization in symptomatic and presymptomatic Huntington's disease, Res Publ Assoc Res Nerv Ment Dis 63 (1985) 199–209.
[11] T. Kuwert, H.W. Lange, K.J. Langen, H. Herzog, A. Aulich, L.E. Feinendegen, Cortical and subcortical glucose consumption measured by PET in patients with Huntington's disease, Brain 113 (Pt 5) (1990) 1405–1423.
[12] W.J. Koroshetz, B.G. Jenkins, B.R. Rosen, M.F. Beal, Energy metabolism defects in Huntington's disease and effects of coenzyme Q10, Ann Neurol 41 (1997) 160–165.
[13] F. Mastrogiacomo, J. LaMarche, S. Dozic, G. Lindsay, L. Bettendorff, Y. Robitaille, L. Schut, S.J. Kish, Immunoreactive levels of alpha-ketoglutarate dehydrogenase subunits in Friedreich's ataxia and spinocerebellar ataxia type 1, Neurodegeneration 5 (1996) 27–33.
[14] T. Matsuishi, T. Sakai, E. Naito, S. Nagamitsu, Y. Kuroda, H. Iwashita, H. Kato, Elevated cerebrospinal fluid lactate/pyruvate ratio in Machado–Joseph disease, Acta Neurol Scand 93 (1996) 72–75.
[15] R.J. Ferrante, Mouse models of Huntington's disease and methodological considerations for therapeutic trials, Biochim Biophys Acta 1792 (2009) 506–520.
[16] W.R. Ellington, T. Suzuki, Early evolution of the creatine kinase gene family and the capacity for creatine biosynthesis and membrane transport, Subcell Biochem 46 (2007) 17–26.
[17] D.M. Dawson, H.M. Eppenberger, N.O. Kaplan, Creatine kinase: evidence for a dimeric structure, Biochem Biophys Res Commun 21 (1965) 346–353.
[18] P. Venkataraman, G. Krishnamoorthy, K. Selvakumar, J. Arunakaran, Oxidative stress alters creatine kinase system in serum and brain regions of polychlorinated biphenyl (Aroclor 1254)-exposed rats: protective role of melatonin, Basic Clin Pharmacol Toxicol 105 (2009) 92–97.
[19] E.C. Stack, W.R. Matson, R.J. Ferrante, Evidence of oxidant damage in Huntington's disease: translational strategies using antioxidants, Ann N Y Acad Sci 1147 (2008) 79–92.
[20] M. Tachikawa, M. Fukaya, T. Terasaki, S. Ohtsuki, M. Watanabe, Distinct cellular expressions of creatine synthetic enzyme GAMT and creatine kinases uCK-Mi and CK-B suggest a novel neuron-glial relationship for brain energy homeostasis, Eur J Neurosci 20 (2004) 144–160.
[21] N.W. Kowall, R.J. Ferrante, J.B. Martin, Patterns of cell loss in Huntington's disease, Trends Neurosci 10 (1987) 24–29.
[22] M. Perluigi, H.F. Poon, W. Maragos, W.M. Pierce, J.B. Klein, V. Calabrese, C. Cini, C. De Marco, D.A. Butterfield, Proteomic analysis of protein expression and oxidative modification in r6/2 transgenic mice: a model of Huntington disease, Mol Cell Proteomics 4 (2005) 1849–1861.
[23] E.C. Stack, J.K. Kubilus, K. Smith, K. Cormier, S.J. Del Signore, E. Guelin, H. Ryu, S.M. Hersch, R.J. Ferrante, Chronology of behavioral symptoms and neuropathological sequela in R6/2 Huntington's disease transgenic mice, J Comp Neurol 490 (2005) 354–370.
[24] J.P. Vonsattel, R.H. Myers, T.J. Stevens, R.J. Ferrante, E.D. Bird, E.P. Richardson Jr., Neuropathological classification of Huntington's disease, J Neuropathol Exp Neurol 44 (1985) 559–577.
[25] L.B. Menalled, J.D. Sison, I. Dragatsis, S. Zeitlin, M.F. Chesselet, Time course of early motor and neuropathological anomalies in a knock-in mouse model of Huntington's disease with 140 CAG repeats, J Comp Neurol 465 (2003) 11–26.
[26] O. Braissant, C. Bachmann, H. Henry, Expression and function of AGAT, GAMT and CT1 in the mammalian brain, Subcell Biochem 46 (2007) 67–81.
[27] S. Stockler, P.W. Schutz, G.S. Salomons, Cerebral creatine deficiency syndromes: clinical aspects, treatment and pathophysiology, Subcell Biochem 46 (2007) 149–166.
[28] O. Braissant, E. Beard, C. Torrent, H. Henry, Dissociation of AGAT, GAMT and SLC6A8 in CNS: relevance to creatine deficiency syndromes, Neurobiol Dis 37 (2010) 423–433.
[29] S.P. Bessman, C.L. Carpenter, The creatine–creatine phosphate energy shuttle, Annu Rev Biochem 54 (1985) 831–862.
[30] R.A. Meyer, H.L. Sweeney, M.J. Kushmerick, A simple analysis of the "phosphocreatine shuttle", Am J Physiol 246 (1984) C365–377.
[31] R.M. Tombes, B.M. Shapiro, Metabolite channeling: a phosphorylcreatine shuttle to mediate high energy phosphate transport between sperm mitochondrion and tail, Cell 41 (1985) 325–334.
[32] E. Van Brussel, J.J. Yang, M.W. Seraydarian, Isozymes of creatine kinase in mammalian cell cultures, J Cell Physiol 116 (1983) 221–226.
[33] F. Streijger, F. Oerlemans, B.A. Ellenbroek, C.R. Jost, B. Wieringa, C.E. Van der Zee, Structural and behavioural consequences of double deficiency for creatine kinases BCK and UbCKmit, Behav Brain Res 157 (2005) 219–234.
[34] H.J. in 't Zandt, W.K. Renema, F. Streijger, C. Jost, D.W. Klomp, F. Oerlemans, C.E. Van der Zee, B. Wieringa, A. Heerschap, Cerebral creatine kinase deficiency influences metabolite levels and morphology in the mouse brain: a quantitative in vivo 1H and 31P magnetic resonance study, J Neurochem 90 (2004) 1321–1330.
[35] S.M. Hersch, H.D. Rosas, R.J. Ferrante, Neuropathology and pathophysiology of Huntington's disease, in: R.L. Watts, W. Koller (Eds.), Movement disorders: neurological principles and practice, McGraw-Hill Professional, 2004, pp. 603–629.
[36] M. Damiano, L. Galvan, N. Deglon, E. Brouillet, Mitochondria in Huntington's disease, Biochim Biophys Acta 1802 (2010) 52–61.
[37] S.M. Henley, G.P. Bates, S.J. Tabrizi, Biomarkers for neurodegenerative diseases, Curr Opin Neurol 18 (2005) 698–705.
[38] S.M. Hersch, S. Gevorkian, K. Marder, C. Moskowitz, A. Feigin, M. Cox, P. Como, C. Zimmerman, M. Lin, L. Zhang, A.M. Ulug, M.F. Beal, W. Matson, M. Bogdanov, E. Ebbel, A. Zaleta, Y. Kaneko, B. Jenkins, N. Hevelone, H. Zhang, H. Yu, D. Schoenfeld, R. Ferrante, H.D. Rosas, Creatine in Huntington disease is safe, tolerable, bioavailable in brain and reduces serum 8OH2'dG, Neurology 66 (2006) 250–252.
[39] K.M. Smith, S. Matson, W.R. Matson, K. Cormier, S.J. Del Signore, S.W. Hagerty, E.C. Stack, H. Ryu, R.J. Ferrante, Dose ranging and efficacy study of high-dose coenzyme Q10 formulations in Huntington's disease mice, Biochim Biophys Acta 1762 (2006) 616–626.
[40] M.B. Bogdanov, O.A. Andreassen, A. Dedeoglu, R.J. Ferrante, M.F. Beal, Increased oxidative damage to DNA in a transgenic mouse model of Huntington's disease, J Neurochem 79 (2001) 1246–1249.
[41] R.J. Ferrante, S.E. Browne, L.A. Shinobu, A.C. Bowling, M.J. Baik, U. MacGarvey, N.W. Kowall, R.H. Brown Jr., M.F. Beal, Evidence of increased oxidative damage in both sporadic and familial amyotrophic lateral sclerosis, J Neurochem 69 (1997) 2064–2074.
[42] M. Bogdanov, W.R. Matson, L. Wang, T. Matson, R. Saunders-Pullman, S.S. Bressman, M. Flint Beal, Metabolomic profiling to develop blood biomarkers for Parkinson's disease, Brain 131 (2008) 389–396.
[43] M. Bogdanov, R.H. Brown, W. Matson, R. Smart, D. Hayden, H. O'Donnell, M. Flint Beal, M. Cudkowicz, Increased oxidative damage to DNA in ALS patients, Free Radic Biol Med 29 (2000) 652–658.
[44] N. Aguirre, M.F. Beal, W.R. Matson, M.B. Bogdanov, Increased oxidative damage to DNA in an animal model of amyotrophic lateral sclerosis, Free Radic Res 39 (2005) 383–388.
[45] C. Isobe, T. Abe, Y. Terayama, Levels of reduced and oxidized coenzyme Q-10 and 8-hydroxy-2'-deoxyguanosine in the CSF of patients with Alzheimer's disease demonstrate that mitochondrial oxidative damage and/or oxidative DNA damage contributes to the neurodegenerative process, J Neurol 257 (2010) 399–404.
[46] M.Y. Heng, P.J. Detloff, R.L. Albin, Rodent genetic models of Huntington disease, Neurobiol Dis 32 (2008) 1–9.
[47] S.M. Hersch, R.J. Ferrante, Translating therapies for Huntington's disease from genetic animal models to clinical trials, NeuroRx 1 (2004) 298–306.
[48] M. Wyss, O. Braissant, I. Pischel, G.S. Salomons, A. Schulze, S. Stockler, T. Wallimann, Creatine and creatine kinase in health and disease—a bright future ahead? Subcell Biochem 46 (2007) 309–334.
[49] E. O'Gorman, G. Beutner, M. Dolder, A.P. Koretsky, D. Brdiczka, T. Wallimann, The role of creatine kinase in inhibition of mitochondrial permeability transition, FEBS Lett 414 (1997) 253–257.
[50] A.M. Klein, R.J. Ferrante, The neuroprotective role of creatine, Subcell Biochem 46 (2007) 205–243.
[51] N. Brustovetsky, T. Brustovetsky, J.M. Dubinsky, On the mechanisms of neuroprotection by creatine and phosphocreatine, J Neurochem 76 (2001) 425–434.
[52] P. Klivenyi, N.Y. Calingasan, A. Starkov, I.G. Stavrovskaya, B.S. Kristal, L. Yang, B. Wieringa, M.F. Beal, Neuroprotective mechanisms of creatine occur in the absence of mitochondrial creatine kinase, Neurobiol Dis 15 (2004) 610–617.